



THE UNIVERSITY *of* EDINBURGH

Edinburgh Research Explorer

Silica cycling and isotopic composition in northern Marguerite Bay on the rapidly-warming western Antarctic Peninsula

Citation for published version:

Annett, AL, Henley, SF, Venables, HJ, Meredith, MP, Clarke, A & Ganeshram, RS 2017, 'Silica cycling and isotopic composition in northern Marguerite Bay on the rapidly-warming western Antarctic Peninsula', *Deep Sea Research Part II: Topical Studies in Oceanography*, vol. 139, pp. 132-142.
<https://doi.org/10.1016/j.dsr2.2016.09.006>

Digital Object Identifier (DOI):

[10.1016/j.dsr2.2016.09.006](https://doi.org/10.1016/j.dsr2.2016.09.006)

Link:

[Link to publication record in Edinburgh Research Explorer](#)

Document Version:

Peer reviewed version

Published In:

Deep Sea Research Part II: Topical Studies in Oceanography

Publisher Rights Statement:

© 2016 Elsevier Ltd. All rights reserved.

General rights

Copyright for the publications made accessible via the Edinburgh Research Explorer is retained by the author(s) and / or other copyright owners and it is a condition of accessing these publications that users recognise and abide by the legal requirements associated with these rights.

Take down policy

The University of Edinburgh has made every reasonable effort to ensure that Edinburgh Research Explorer content complies with UK legislation. If you believe that the public display of this file breaches copyright please contact openaccess@ed.ac.uk providing details, and we will remove access to the work immediately and investigate your claim.



Title: Silica cycling and isotopic composition in northern Marguerite Bay on the rapidly-warming western Antarctic Peninsula

Authors: Amber L. Annett^{*1}, Sian F. Henley¹, Hugh J. Venables², Michael P. Meredith², Andrew Clarke², Raja S. Ganeshram¹

¹School of Geosciences, University of Edinburgh, UK

²British Antarctic Survey, Cambridge, UK

^{*}Corresponding author: A. L. Annett, School of GeoSciences, The Grant Institute, The King's Buildings, University of Edinburgh, James Hutton Road, Edinburgh UK, EH9 3FE. Present address: Department of Marine and Coastal Sciences, Rutgers University, 71 Dudley Road, New Brunswick, NJ, USA, 08901. (annett@marine.rutgers.edu)

Abstract:

The Southern Ocean is a key region for silica (Si) cycling, and the isotopic signatures established here influence the rest of the world's oceans. The climate and ecosystem of the Southern Ocean are changing rapidly, with the potential to impact Si cycling and isotope dynamics. This study examines high-resolution time-series dataset of dissolved Si concentrations and isotopic signatures, particulate Si concentrations and diatom speciation at a coastal site on the western Antarctic Peninsula (WAP), in order to characterise changes in Si cycling with respect to changes occurring in productivity and diatom assemblages. Dissolved and particulate Si phases reflect the dominant control of biological uptake, and combined with isotopic fractionation were consistent with a season of low/intermediate productivity.

Biogenic Si is tightly coupled to both chlorophyll and particulate organic carbon at the sampling site, consistent with diatom-dominated phytoplankton assemblages along the WAP. Variability in diatom speciation has a negligible impact on the isotopic signature of dissolved Si in surface waters, although this is unlikely to hold for sediments due to differential dissolution of diatom species. A continued decline in diatom productivity along the WAP would likely result in an increasing unused Si inventory, which can potentially feed back into Si-limited areas, promoting diatom growth and carbon drawdown further afield.

1. Introduction:

The shelf regions of the Southern Ocean are characterised by weak stratification and high productivity, and consequently play a major role in the biological pump of carbon by affecting the air-sea balance of CO₂ and the export of organic carbon (C) to deep waters (Sarmiento et al., 2004, 2007). This area is also of great significance to the marine silica (Si) cycle (de Souza et al., 2014) as the dominant phytoplankton group is diatoms; these take up silica to form siliceous frustules and account for up to 75% of primary production (Nelson et al., 1995). The high productivity, abundant Si and robust diatom communities lead to extensive siliceous sediment deposits between the Antarctic Polar Front (APF) and the marginal sea-ice zone to the south. North of the APF, however, availability of Si is low and likely limits diatom production throughout most or all of the growing season (Nelson et al., 2001). As a result of iron limitation, which leads to increased Si:N ratios in iron-limited diatoms (Marchetti and Cassar 2009), Si is preferentially depleted with respect to N and P as surface waters move northward across the APF. This separates the supply of the macronutrients, and the preferential depletion of Si has global impacts as these waters supply nutrients to much of the world's surface oceans via formation of Southern Ocean mode and intermediate waters (Rintoul and Trull 2001, Brzezinski et al., 2002, Sarmiento et al., 2004, 2007, de Souza et al., 2014). The reduced supply of Si relative to other nutrients limits diatoms to a relatively minor role in most other oceanic provinces (Yool and Tyrell 2003). Changes in the export of Si from the Southern Ocean and resulting increases in diatoms at low latitudes have been proposed as a mechanism to alter atmospheric CO₂ at glacial-interglacial time scales (Brzezinski et al., 2002, Matsumoto et al., 2002, Hendry et al., 2014a). Accordingly, understanding Si supply to the Southern Ocean and diatom use thereof is important in constraining both current oceanic productivity as well as reconstructing past nutrient use from sediment records.

The western Antarctic Peninsula (WAP) region is one where warm, nutrient-rich Upper Circumpolar Deep Water (UCDW) intrudes onto the shelf and can upwell/mix up to influence the surface layers (Martinson et al., 2008). The lack of a strong shelf-break front adjacent to the western edge of the peninsula (Jacobs 1991, Whitworth et al., 1998) allows WAP waters to exchange with those of the off-shelf Antarctic Circumpolar Current (ACC), making the WAP a source region supplying nutrients to the surface Southern Ocean. As such, changes along the WAP have the potential to affect Si supply and use on a significant spatial

scale. In addition, the WAP has experienced the most rapid regional climate change in the southern hemisphere over recent decades (Vaughan et al., 2003). Air and surface water temperatures have increased dramatically (Vaughan et al., 2003; Meredith and King 2005), and sea-ice dynamics have shifted to later advance and earlier retreat, resulting in a significantly shorter ice-covered period (Massom and Stammerjohn 2010) and deeper winter mixing (Venables et al., 2013). Significant biological changes have also been observed, with lower chlorophyll *a* concentrations along the WAP as a whole (Montes-Hugo et al., 2009) and effects on grazers such as krill (Loeb et al., 1997; Atkinson et al., 2004), and higher trophic levels (Saba et al., 2014).

Against the background of rapid ongoing changes in physical conditions and biological processes at the WAP, this study examines the concentration and isotopic signature of dissolved Si (Si_d) at high resolution during the summer growing season of 2009-2010 in Ryder Bay, the site of the Rothera Oceanographic and Biological Time Series (RaTS; Clarke et al., 2008). Biological uptake favours the lighter ^{28}Si isotope, leaving the remaining reactant pool and product progressively enriched in ^{29}Si and ^{30}Si as drawdown progresses. In diatoms, Si_d is actively transported into the cell to meet cellular requirements for biogenic silica (SiO_2 ; hereafter “BSi”; Hildebrand 2008). Thus, the isotopic signature associated with diatom Si use has shown considerable potential as a proxy for both current Si cycling (Varela et al., 2004, Cardinal et al., 2007, Beucher et al., 2011, Fripiat et al., 2011) and paleoceanographic Si processes (De La Rocha et al., 1998, Beucher et al., 2007, Pichevin et al., 2009, Ellwood et al., 2010, Pichevin et al., 2012, Hendry et al., 2014b). This is especially important in the Southern Ocean, where calcareous organisms are scarce and thus the widely-used proxies based on calcareous sediments are less useful than in low-latitude regions.

Questions remain in our understanding of the processes controlling Si fractionation, however. Chief among these are the effects of temperature and diatom speciation on Si fractionation in oceanographically-relevant conditions. Increasing incorporation of Si concentrations and isotopic data in modelling studies (Gnanadesikan and Toggweiler 1999, Wischmeyer et al., 2003, Reynolds 2009) requires an understanding of the fractionation associated with biological uptake throughout the world, but especially at the low temperatures typical of the Southern Ocean where Si availability is high and polar diatom species dominate. A separate paper analyses mixing and drawdown aspects of the Si system at the WAP (Cassarino et al., this issue); here we focus on coupling *in-situ* time-series

96 measurements of the isotopic composition of the Si_d pool with high-resolution diatom species
97 data. These complementary records are used to investigate the effects of changing diatom
98 speciation on Si isotopic signatures in the ocean. Further, a seasonal Si budget is derived for
99 Ryder Bay, to assess variations in Si-use in the context of current climate change.
100

2. Methods:

2.1 Oceanographic context

Ryder Bay is a shallow (520 m) embayment at the northern end of Marguerite Bay, Adelaide Island, and the site of the long-running RaTS programme. Conditions are generally typical of an Antarctic seasonal sea-ice zone, with winter ice cover varying considerably from <40 to >120 days (Venables et al., 2013). Over winter, a cold and saline water mass is formed (termed winter water, “WW”), reaching maximum depths of ~50 to >150 m depending upon the duration of ice cover (Venables et al., 2013). The deep source for WW is Circumpolar Deep Water, which intrudes onto the Antarctic Peninsula shelf in relatively unmodified form (Klinck 1998). During the course of the summer, warming and freshening due to insolation and freshwater inputs create an increasingly stratified upper water column, with Antarctic Surface Water (AASW) as the topmost layer. Meteoric water (glacial melt and precipitation) accounts for up to ~6% of the water column in summer, compared to around -2 to 2% melt from sea ice (where negative values denote net sea ice formation), though interannual variability in each of the freshwater components is large (Meredith et al., 2010).

Stratified summer conditions (Venables et al., 2013), along with high macro- and micro-nutrient concentrations support intense summer productivity (Clarke et al., 2008, Annett et al., 2015, Henley et al., this issue), a common feature of seasonally ice-covered coastal waters. In Ryder Bay and the WAP as a whole, phytoplankton communities are dominated by diatoms (Holm-Hansen et al., 1989; Varela et al., 2002; Clarke et al., 2008; Annett et al., 2010).

As part of the long-term oceanographic monitoring of the RaTS programme, a suite of physical, biogeochemical and biological data is available from the British Antarctic Survey (Cambridge, UK). These data include hydrographic conditions (temperature, salinity, etc.) and biological activity (*i.e.* chlorophyll and nutrient concentration). Detailed methodology used by this programme for CTD data collection and chlorophyll/nutrient analysis can be found in Clarke et al., (2008).

2.2 Sample collection

Samples for surface water Si_d and BSi analyses were collected from RaTS sites 1 and 2 in Ryder Bay, Adelaide Island, Antarctica (Figure 1), during austral summer 2009 (December 2009 – March 2010). The primary sampling site is situated ~4 km from the coast, with local

maximum water depth of 520 m. When weather or brash ice prevented access to site 1, site 2 (~400 m depth) was used; compatibility of this alternative sampling site, representative of the processes at work in Ryder Bay, has been established (Clarke et al., 2008). Previous work has shown the primary oceanographic source for Ryder Bay to be inflow of water masses from northern Marguerite Bay, with some local modification from glacial melt and topographically-related processes (Clarke et al., 2008; Venables and Meredith 2014; Wallace et al., 2008). Marguerite Bay in turn has been shown to display physical water mass characteristics similar to the inshore part of the WAP region as a whole (Meredith et al., 2004, Venables and Meredith 2014).

RaTS sampling occurs approximately twice weekly in summer and weekly in winter, with Conductivity-Temperature-Depth (CTD) casts conducted to nearly the full depth of the water column. In addition, discrete samples are collected with a Niskin bottle from 15 m, the long-term average depth of the chlorophyll *a* maximum (Clarke et al., 2008). For the present study, additional samples were collected from 0, 5, 10 and 25 m depth on a weekly basis, weather permitting. Deeper waters (50, 100 and 500 m) were sampled approximately monthly for other parameters (N isotopes; Henley et al., this issue), and small volumes (~125 ml) were collected for Si_d concentration and isotopic analysis whenever possible. Deep water was collected using a 5 l Niskin bottle and surface water (≤25 m) was collected using a submersible Whale pump attached to 32 mm diameter silicone tubing and powered by a portable 13 V battery. Tubing was cleaned with 10% v/v HCl (reagent grade) and ultra-pure water (Milli-Q: 18MΩ, Millipore® systems) in the laboratory, and ~25 l of *in situ* seawater at each depth before sample collection. The flow rate of the pump was kept at 5–8 l min⁻¹ to prevent settling of particles during collection. Samples were transported back to the laboratory in the dark in 20 l carboys or 125 ml bottles.

Particulate samples for BSi analysis were collected in 2009, and also in summer 2008 (December 2008 – March 2009), for which sample collection, processing and analysis were identical to the 2009 samples. Particulates from 1 l of water were collected onto acid-cleaned (10% v/v HCl, Aristar grade) 47 mm polycarbonate membrane filters (0.6 μm). Filters were dried overnight at ~40 °C in PetriSlides and kept at room temperature until analysis. Duplicate samples of filtrate (10 ml) were collected into centrifuge tubes for analysis of both Si_d concentration and isotopic signature (δ³⁰Si_d). Dissolved samples were acidified with 1 ml l⁻¹ of 50% v/v HCl (Aristar grade) to prevent bacterial activity and stored at room

temperature. All plastic ware for sample collection, filtration and storage was acid-cleaned (10% v/v HCl, Aristar grade) for at least 24 h and rinsed thoroughly with Milli-Q before use.

Samples for diatom species analysis were collected from pump outflow, stored in 250 ml amber glass bottles, and preserved with 2.5% Lugol's fixative (iodine solution) which was lowered to pH <7 to prevent dissolution of silica. Samples were stored in the dark at 4°C until they were filtered (~2–24 hours after collection). Volumes of 50–100 ml were filtered gently onto 25 mm, Millipore® HAWG (0.45 µm) filters, which were then covered with foil and dried overnight in an oven at low temperature (37 °C). The dry filters were mounted on slides using microscope immersion oil and gentle heating, according to the methods in the Millipore® catalogue (Cat. No. LAB310/P).

On 23 January 2010, full-depth water column sampling was undertaken at the RaTS site as well as two locations in Marguerite Bay at -67° 52.44 S, -68° 05.69 E and -67° 44.70 S, -68° 08.33 E (termed MB1 and MB2, respectively). This was possible by sampling from the ARSV *Laurence M. Gould*, during a CTD cross-calibration between RaTS and the Palmer Long-Term Ecological Research programs. Samples from Niskin bottles deployed on the ship's rosette were collected into 4 l acid-washed bottles, and stored in the dark during return to the laboratory at Rothera Station. Further processing of these samples for Si_d concentration and isotopic signature and BSi followed the methods above for all RaTS samples.

2.3 Processing

2.3.1 Dissolved Si concentration

Concentration of dissolved Si was determined spectrophotometrically using HACH® reagents (Silica Reagent Set, Ultra Low Range, Bulk Solution), following the manufacturer's directions. This method is based on the formation of a blue silicomolybdate complex, which can be assessed quantitatively by measuring absorbance at 812 nm in a 1 cm cell. Samples of 1 ml were diluted with 2 ml Milli-Q to prevent interference from the saltwater matrix, which was < 5% at this dilution level (results not shown). Samples were analysed in duplicate and where variation was >10%, additional duplicate samples were also measured.

2.3.2 Dissolved Si isotopic composition

Silicon isotopic composition ($\delta^{30}\text{Si}$) is expressed as the difference between the ratios of heavy (^{30}Si) to light (^{28}Si) atoms in a sample versus a standard reference material (in this case quartz standard NBS28), according to the equation:

$$\delta^{30}\text{Si}_{\text{sample}} = \frac{\left(\frac{^{30}\text{Si}_{\text{sample}}}{^{28}\text{Si}_{\text{sample}}} - \frac{^{30}\text{Si}_{\text{std}}}{^{28}\text{Si}_{\text{std}}} \right)}{\frac{^{30}\text{Si}_{\text{std}}}{^{28}\text{Si}_{\text{std}}}} \times 1000 \quad (1)$$

with results expressed in permil (‰) notation.

Isotopic composition of dissolved Si ($\delta^{30}\text{Si}_d$) was analysed following the method of Reynolds et al., (2006) with modifications by de Souza et al., (2012) prior to analysis by High-Resolution Multi-Collector Inductively-Coupled-Plasma (HR-MC-ICP) mass spectrometry. Briefly, Si was pre-concentrated by the addition of NaOH. As fractionation can occur during precipitation, complete recovery of Si is essential to prevent any effects on the $\delta^{30}\text{Si}_d$ signature (Cardinal et al., 2005, Reynolds et al., 2006). All samples analysed had >98% recovery. Concentrated samples were purified on Bio-RAD AG-50W-X8 resin, and eluted to give a final volume of 5 mL and Si_d of 1 ppm.

Purified Si samples were analysed for $^{30}\text{Si}/^{28}\text{Si}$ and $^{29}\text{Si}/^{28}\text{Si}$ ratios on a Nu1700 HR-MC-ICP mass spectrometer at ETH-Zürich, with a Nu Instruments DSN desolvator and a PFA nebuliser. Standards used were NBS28 and Diatomite reference material. Measurements were made using standard-sample-standard bracketing, with 5–9 replicate measurements for each sample, giving 95% confidence limits of <0.12 ‰ (2 standard deviations <0.25 ‰). Full details of the mass spectrometry methods are given in Georg et al., (2006).

2.3.3 Particulate Si concentration

Concentration of particulate BSi was determined using an adaptation of the double wet-alkaline digestion outlined by Ragueneau and Treguer (1994), based on a method proposed by Brzezinski and Nelson (1989). Corrections were made for lithogenic contamination from Al:Si ratios as developed by Ragueneau et al., (2005). Due to the higher suspended particulate matter concentrations in Ryder Bay samples, the method was modified by increasing digestion time to 60 min, and extraction volumes were 4 ml for most samples (as in Ragueneau et al., 2005) but 8 or 10 ml for high-particulate samples, to avoid any Si loss through precipitation.

Dissolved Si and Al were determined using a Varian VISTA Pro ICP–OES (Axial) in the School of Geosciences, University of Edinburgh (UK). A background solution of NaOH

plus HCl replicated the concentrations used in the extraction and neutralisation steps, to eliminate any matrix effects from high Na content. Samples were run using an AutoAnalyser, with 5 replicate peak measurements for each element, and internal standards of In, Bi, Sc and Y. Regression of the standard calibration curves were highly linear, with r^2 values above 0.95 for each element measured. For most samples the Si:Al ratio in the second extraction was ~5.6 mol:mol, therefore any samples where Si:Al exceeded 8 mol:mol were subjected to a third extraction to ensure that elevated Si:Al due to residual BSi could be accounted for.

For comparison to previous seasons with different environmental conditions, data are also available from particulate samples collected at 15 m in the summers of 2004 and 2005, and analysed previously by X-Ray Fluorescence (XRF; of particulate matter collected on polycarbonate membrane filters, full details in Carson 2008). These earlier data are total particulate Si (Si_T), in contrast to the 2008-2010 data that are BSi.

2.3.4 Diatom species composition

Diatom counts were performed using a Leica microscope at 500x magnification. The HAWG filters are pre-printed with grid squares of 9.50 mm², and phytoplankton were enumerated and identified in three randomly-chosen grid squares. Cells were identified to species, genus or group level (as possible), using the taxonomic guidelines outlined in Hasle and Syvertsen (1997). In the event that less than 300 cells were enumerated in three grid squares, additional squares were counted until the cell total exceeded 300. Counts were combined with the fraction of the filter area scanned and the volume filtered to convert these to cell concentrations per ml of seawater. For very large species (e.g. *Coscinodiscus* spp), additional squares were scanned and counted only for these species, and abundances for these species calculated based on the larger filter area analysed.

Due to the large range in diatom cell volume, interspecific comparisons of cellular concentrations (cells l⁻¹) are an imprecise or even inadequate method of characterising phytoplankton communities (Smayda 1978). Cell volume estimates were made to facilitate estimates of biomass, using geometric formulae appropriate to the shape of the cell (Smayda 1978, Hillebrand et al., 1999) and cell measurements from digital images. Full methods of conversion from cell volume to biomass as well as cell shapes used are given in Annett et al., (2010) and Annett (2013).

3. Results:

3.1 Oceanography

Water column conditions at the RaTS site are influenced by winter mixing and the stratifying effects of summer insolation, sea-ice melt, and freshwater input from glacial ice and snow melt. Winter 2009 exhibited a mixed layer depth (MLD, defined here as the depth at which potential density exceeds that of surface water by 0.05 kg m^{-3} ; Clarke et al., 2008) of $>75 \text{ m}$, followed by a marked transition to shallower depths in late November (Figure 2a). With the exception of one mixing event in mid-December, the MLD remained shallow throughout the growing period, deepening into April. The formation of warmer, less saline AASW is clear in the temperature profiles in Figure 2b, overlying the colder WW, and modified Circumpolar Deep Water (mCDW) present below $\sim 200 \text{ m}$.

Stratified, well-lit surface waters allow for phytoplankton growth, and chlorophyll concentrations at 15 m show a short-lived increase in early December and a longer-lived bloom in February (Figure 2a). Overall, biological activity during this period was lower than is typical for this site. Average and peak chlorophyll were 6.3 ± 5.0 and 20 mg m^{-3} , respectively, compared to higher-chlorophyll seasons (e.g. summer 2004 and 2005; Venables et al., 2013), where average chlorophyll is 10 to 15 mg m^{-3} and peaks were above 24 mg m^{-3} . However, in some recent years chlorophyll concentrations have been even lower (e.g. 2007, average and peak concentrations of 1.70 and 3.95 mg m^{-3} , respectively). Thus the season examined here is considered an intermediate-chlorophyll year within the context of variability at the RaTS site.

3.2 Surface and deep water Si_d

At 15 m , Si_d shows a trend of moderate drawdown of $\sim 0.112 \mu\text{M d}^{-1}$ during the sampling period, with relatively consistent concentrations throughout the surface waters (to 25 m , Figure 3a, b). Initial Si_d was $\sim 45 \mu\text{M}$, but increases throughout the profile by $\sim 5 \mu\text{M}$ at the end of December. Gradual depletion then occurs throughout the water column until early March, when concentrations show a slight increase as winter mixing begins.

Deep waters are significantly enriched in Si_d relative to surface waters, with maximum concentrations $>80 \mu\text{M}$ (Figure 3b). A gradual increase in Si_d in deep water can be seen over the course of the season at $\sim 200 \text{ m}$. One sampling event allowed collection of depth profile samples from the RaTS site, and two locations in Marguerite Bay (Figure 3d). These data

show that Si_d is highly consistent at the three locations, in agreement with previous studies that indicate waters of Ryder Bay to be broadly representative of conditions in Marguerite Bay (Venables and Meredith 2014). The increase in Si_d with depth to a maximum concentration of $\sim 80 \mu M$, seen in the Ryder Bay time series, is also seen in Marguerite Bay including the deeper waters at station MB1 (620 m water depth).

3.3 Particulate biogenic Si

In agreement with a small chlorophyll bloom that began prior to sampling, BSi was initially high, but declined into January (Figure 3c). The late-season chlorophyll peak is concurrent with BSi increasing from mid-January to a maximum of $\sim 9 \mu M$ in mid-February. BSi was also measured in the top 25 m of the water column, as for dissolved samples, and trends from 15 m water samples were found to be largely representative of the surface waters as a whole, with slightly higher BSi found at 0–10 m on two occasions.

3.4 Isotopic composition of Si_d

Consistent with the moderate drawdown of Si_d , there is a slight, gradual enrichment in $\delta^{30}Si_d$ from January to March (Figure 4a; 0.0034 ‰ d^{-1} ; p -value 0.012), after the period of low chlorophyll in late December/early January (Figure 2). Early season (late December, after the early bloom) samples were $\sim 1.6 \text{ ‰}$, but increased to $\sim 2.0 \text{ ‰}$ by March 2010. Deep (100–110 m) samples showed lighter isotopic signatures (100m versus 15 m samples, p -value < 0.03 , two-sample t-test). Heavier values late in the season were also observed in the deep samples, which may be a reflection of surface water being mixed downwards as stratification breaks down in austral fall.

Five samples were collected from deeper waters on 23 Jan 2010, in order to investigate isotopic signatures below the WW layer. These were collected from 200, 280, 350, 446 and 496 m, where bottom depth was ~ 500 m. These samples gave values ranging from 0.81 to 1.0 ‰, with the lightest value at the deepest depth (Figure 4b). A composite depth profile including most of the samples from the season (excluding the late-season 100 m sample, which displayed very high $\delta^{30}Si_d$) highlights the trend towards heavier surface values, consistent with preferential biological uptake of lighter isotopes in the euphotic zone.

3.5 Diatom biomass composition

Biomass of the ten main diatom groups at 15 m show a pattern of seasonal succession (Figure 5). Early in the season small, chain-forming *Chaetoceros* spp. dominated, and from mid-December through January *Proboscia inermis* accounted for most of the biomass. Large centric species were abundant in February, with other groups also making significant contributions. Towards the end of the season *Eucampia antarctica* biomass increased to up to 50% of the total, with the final sample heavily dominated by the *Coscinodiscus* genus of very large diatoms.

4. Discussion:

4.1 Silica cycling and isotope dynamics

Similar to most of the Southern Ocean, the surface waters in Ryder Bay have Si_d values that are relatively high, ranging from 35–60 μM . Long-term average patterns from the full RaTS series show a seasonal cycle with winter concentrations of $\sim 65 \mu\text{M}$ gradually decreasing throughout the summer to a minimum of $<40 \mu\text{M}$ in March (Clarke et al., 2008, Henley et al., this issue). The data from this study show the same pattern of slow decline through the summer season. While these data suggest that winter replenishment was lower than average immediately prior to summer 2009, our sampling missed the initial increase in chlorophyll (Figure 2) and BSi (Figure 3), thus the early season Si_d is likely to have been higher than the first samples collected here. In agreement, records indicate winter Si_d of almost 80 μM in early November (British Antarctic Survey, and Henley et al., this issue).

The concentration of BSi at 15 m displays a bi-modal seasonal pattern (Figure 3), typical of chlorophyll in this area (Clarke et al., 2008). The mid-December increase in Si_d , and decreases in BSi and $\delta^{30}\text{Si}_d$, correspond to a deeper mixed layer (to $\sim 50 \text{ m}$; not shown; data from BAS). This replenishes surface Si by entraining some high-Si, low- $\delta^{30}\text{Si}_d$ water into the surface layer and diluting BSi and chlorophyll, resulting in this bi-modal pattern (Figure 3). Periods of higher BSi are coincident with lower Si_d , reflecting uptake of Si into the particulate phase as a result of biological production. Phytoplankton biomass is generally dominated by diatoms (mean 78 % of total phytoplankton biomass; Annett et al., 2010), and other Si-containing microorganisms (*i.e.* silicoflagellates) are comparatively rare (Annett et al., 2010). In fact, the relationship between Si and both chlorophyll and POC (POC from Henley et al., 2012; Henley 2012) is strong and statistically significant at this site (Figure 6), and it is well established that diatoms dominate phytoplankton communities along the WAP

(Varela et al., 2002, Garibotti et al., 2005, Clarke et al., 2008, Annett et al., 2010). This robust ($r^2 = 0.85$) relationship allows BSi to be estimated from chlorophyll and POC concentrations according to the equations:

$$\text{BSi} = (0.39 \pm 0.018) \times [\text{chl}] + (0.96 \pm 0.20) \quad (2)$$

and

$$\text{BSi} = (0.15 \pm 0.011) \times [\text{POC}] - (0.28 \pm 0.37) \quad (3)$$

Further implications of the tight chlorophyll and POC coupling are discussed in sections 4.4 and 4.5.

Two important trends are evident in the time-series and depth profile values of $\delta^{30}\text{Si}_d$. Firstly, the decrease in Si_d from January to March is accompanied by isotopic enrichment. Compared with surface waters in other regions, this enrichment and drawdown is relatively minor (to minimum $\sim 30 \mu\text{M}$ and $\sim 1.8 \text{‰}$ here, compared to *e.g.* $<1 \mu\text{M}$ and $>3 \text{‰}$ in the North Pacific, Reynolds et al., 2006). Preferential incorporation of lighter isotopes into biogenic material leaves the dissolved reactant pool progressively enriched in the heavier isotopes, thus it is expected that $\delta^{30}\text{Si}_d$ increases with increasing extent of Si utilisation over the course of the growing season. Consequently, the moderate enrichment (from ~ 1.6 to 2.0‰) is consistent with a moderate extent (from ~ 50 to $35 \mu\text{M}$, or 30%) of Si use.

Secondly, deep waters have much higher concentrations of Si_d (up to $80 \mu\text{M}$), and display much lighter $\delta^{30}\text{Si}_d$ values, consistent with deep waters being the source of Si to surface waters. The very light values also suggest that deep water in this region has experienced little utilization, consistent with deeper waters being the primary Si source. The 0.81‰ values at depth are among the lowest reported from the Southern Ocean, consistent with the estimate made for AABW based on deep North Pacific water (0.8‰ ; Reynolds et al., 2006), with low values at depth near the Kerguelen Islands (Fripiat et al., 2011, Coffineau et al., 2014), and with the Southern Ocean being a low- $\delta^{30}\text{Si}_d$ source of Si to the global ocean (de Souza et al., 2014).

The high Si_d and low $\delta^{30}\text{Si}_d$ at depth may also reflect some extent of regenerated Si, as this process may contribute to light isotopic signatures. A study by Demarest et al., (2009) found that remineralisation preferentially releases the light isotopes that have been incorporated into sinking particles (fractionation factor approximately 0.55‰). However, subsequent studies have not found any fractionation associated with remineralisation of BSi

(Wetzel et al., (2014) in experimental conditions; Fripiat et al., (2012) using in situ vertical profiles of BSi; Egan et al., (2012) by comparing $\delta^{30}\text{Si}$ of surface BSi samples and sediments; Varela et al., (2004) and Closset et al., (2015) using the isotopic composition of settling particles), thus any isotopic effect of Si regeneration remains unclear.

Several studies have investigated surface water isotope dynamics with a view to determining if open or closed systems are more appropriate (*e.g.* Varela et al., 2004). In a closed system, the reactant pool is finite and isolated from replenishment, while the product, in this case BSi, accumulates. In an open or steady-state model reactant is continuously supplied, and the product sinks and is lost from the system. For this study, there is a strong regression for both systems (Figure 7). Because of the moderate extent of drawdown (maximum 30%), the theoretical trends for the two systems are very similar over this range of Si_d concentrations, and therefore these data cannot discriminate between the two models.

Of particular significance in the above analyses are the slope values, which in both cases represent the fractionation factor, ϵ . These ϵ estimates are $-1.19 \pm 0.13 \text{ ‰}$ (closed) and $-1.86 \pm 0.20 \text{ ‰}$ (open), in agreement with those found in laboratory and other field studies (*i.e.* De La Rocha et al., 1997, Varela et al., 2004, Sutton et al., 2013). The strong agreement between studies is evidence that Si cycling in Ryder Bay is subject to the same dominant (biological) control as elsewhere in the Southern Ocean.

4.2 Effects of diatom speciation on biological fractionation of Si

A strong relationship exists between Si use and $\delta^{30}\text{Si}_d$ (Figure 7). However, there are some surface water values that display minor deviations from the expected trend. In surface waters, several factors can affect the apparent isotopic fractionation, including temperature, sea-ice material, mixing, or species effects. Temperature is unlikely to have a significant effect here, due to the relatively small temperature range ($\sim 2 \text{ °C}$). Sea ice material is also an unlikely factor, as little to no sea ice was present in Ryder Bay during summer 2009. Dissolution could potentially influence isotopic signatures (Demarest et al., 2009), although most studies have found no isotopic shift associated with dissolution (Egan et al., 2012; Fripiat et al., 2012; Wetzel et al., 2014; Closset et al., 2015). Any fractionation accompanying dissolution would preferentially release the lighter isotope, leading to lighter values in the dissolved phase, and thus cannot account for positive excursions from the expected trend. Similarly, mixing with underlying (lighter) waters is also not able to explain heavier $\delta^{30}\text{Si}_d$.

Of the surface samples, four have high $\delta^{30}\text{Si}_d$ relative to the expected relationship (Figure 7), although we emphasize that these offsets are small and that overall the relationship is strong. The earliest and latest samples (December 2–7 2009 and March 15–18 2010, respectively) show the greatest difference between measured and expected $\delta^{30}\text{Si}_d$ (“residual $\delta^{30}\text{Si}_d$ ”) based on Si_d and the trends shown in Figure 7. We suggest this may be linked to species changes in the diatom community (Figure 5), as the greatest $\delta^{30}\text{Si}_d$ offset values occurred at the end of the season, when there was a large proportion of biomass from a single diatom genus (*Coscinodiscus*). Similarly, *Chaetoceros* (*Hyalochaeta* subgenus) contributed ~30% of diatom biomass in samples with a slight positive offset $\delta^{30}\text{Si}_d$ at the beginning of sampling.

Uptake of Si offers a theoretical basis for species differences in fractionation of Si, although mechanisms of diatom Si uptake remain only partially characterized (reviewed in Martin-Jézéquel et al., 2000, Hildebrand 2008, Thamtrakoln and Hildebrand 2008). Fractionation is dominated by the uptake step (Milligan et al., 2004), responding to changes in Si requirements during different stages of the cell cycle. Factors potentially influencing ϵ include the timing of productivity through the season, and variable life history strategies such as resting spore formation (De La Rocha, 2006). Cells of the subgenus *Hyalochaeta* are known to form heavily silicified *Chaetoceros* resting spores (CRS) early in the growing season in Antarctic waters (Garrison 1984; Leventer et al., 2002). CRS abundance was over 3-fold higher on 7 Dec 2009 than in any other sample (Annett 2013), suggesting resting spore formation may be associated with higher values of ϵ . Indeed, recent culture work found an ϵ of ~ -2.09 ‰ for *Chaetoceros brevis* (Sutton et al., 2013). This greater ϵ would result in particulate matter isotopically lighter than expected, thus leaving the remaining Si_d more enriched (*i.e.* a positive offset) as seen here. Our study also suggests that *Coscinodiscus* spp. may have high ϵ values, although at present no laboratory studies have tested this. We emphasize that the Si_d - $\delta^{30}\text{Si}$ correlation is robust ($r^2 > 0.78$ and $p \ll 0.05$, for both open- and closed-system dynamics), and overall any species effects are minor in surface water samples. While this initially suggests that a species effect is unlikely to be seen at the resolution typically available in sedimentary records, differential dissolution and preservation of diatom species could exaggerate the minor isotopic effects suggested here, leading to significant implications for sediment studies.

Chaetoceros species are often dominant in Southern Ocean sediment cores (as CRS), particularly in coastal areas. In sediment traps from Ryder Bay, CRS accounted for 52% of diatom valves during the 2004 and 2005 summers, compared with an average 12% of surface water diatoms (by abundance; data from Annett et al., 2010, Henley et al., 2012). Thus, disproportionate preservation of this species would be expected to bias sediment records. Higher proportions of CRS, with a lighter particulate $\delta^{30}\text{Si}$ signal than other species, might be interpreted as reflecting lower Si use if a species-specific ϵ is not considered. In agreement, model results of Sutton et al., (2013) suggest that diatom species variation can explain up to 67% of $\delta^{30}\text{Si}$ variation in core records. Such an effect could decouple sediment records from surface waters.

4.3 Isotopic effect of seasonal succession in diatom community and size classes

These data also suggest that some of the species and size dependent differences in $\delta^{30}\text{Si}$ seen in sedimentary layers could be related to the temporal succession of the diatom community over the growing season, and may not be related to species-specific changes in ϵ . For instance, *Chaetoceros* are more abundant early in the season when Si_d shows less depletion and relatively lighter $\delta^{30}\text{Si}_d$, whereas *Odontella weissflogii* peaks later in the season when surface water Si_d shows more depletion and heavier $\delta^{30}\text{Si}_d$ (Figures 4, 5). Differential preservation of these species in sediments could potentially produce large isotopic differences, independent of species changes in ϵ , reflecting seasonal succession during growth. Similarly, large centric diatoms ($> 50 \mu\text{m}$) occur in roughly equal proportion to medium centric species (20-50 μm) during the early season but dominate over medium-sized centrics during the later bloom period (Figures 4, 5). Isolation of the $>50 \mu\text{m}$ diatom fraction for Si isotopic analysis could bias towards heavier $\delta^{30}\text{Si}$ signatures during sedimentary reconstruction. The data presented here suggest that seasonal succession in diatom species and sizes reflecting periods of differing Si depletion can be amplified in sediments by differential dissolution or analytical techniques. Therefore we highlight the need for more work to assess the factors affecting $\delta^{30}\text{Si}$ signatures in both water column and core samples, and the relationship between them, in order to fully validate the use of the $\delta^{30}\text{Si}$ proxy in sedimentary records.

4.4 Silicon budgets in Ryder Bay estimated from isotopic data

Diatoms are a dominant component of WAP productivity, particularly in Ryder Bay (Clarke et al., 2008, Annett et al., 2010), such that Si cycling will largely reflect overall productivity in this region. Here we use concentrations and isotopic measurements to estimate a seasonal Si budget based on overturning of the upper water column (following Fripiat et al., 2011). This approach uses a one-dimensional model of homogenous WW resulting from mixing of two end-members: Si-deplete surface waters following the summer bloom, and Si-rich deep water. Late-season surface waters (depleted source) and deep Ryder Bay water (> 200 m, below the WW layer; Si-rich source) were used as endmembers (Figure 8). If these water masses mix vertically (with negligible horizontal variation at the regional scale), the depletion experienced at the surface during the summer bloom will be balanced by resupply from depth at annual scales. Given the highly consistent Si_d observed from Ryder Bay into Marguerite Bay (Figure 3d), this should be a valid approach for Ryder Bay. If steady state conditions apply at the annual scale (*i.e.* export equals supply), then this vertical supply will be equal to the annual production of BSi.

The fractional contribution of deep Si-rich waters to the WW layer (f_{DEEP}) was calculated following the equation from Fripiat et al., (2011):

$$f_{DEEP} = \frac{\delta^{30}Si_d^{WW} - \delta^{30}Si_d^{SML}}{\delta^{30}Si_d^{DW} - \delta^{30}Si_d^{SML}} \quad (4)$$

where superscripts refer to winter water (WW), summer mixed layer (SML) and deep waters (DW). All values used for this calculation, and rationale for each value choice, are listed in Supplementary information (and table S1). This contribution to WW for 2009 was 0.21. The depth of the winter mixed layer towards the end of winter was 80 m. Integrating winter Si_d (55 μM) over this depth gives a total Si contribution from deep water (to winter water) of 0.93 mol Si m^{-2} . In the summer, the euphotic mixed layer subject to Si drawdown was 30 m. Thus, the amount of WW Si entrained into the surface layer was 0.35 mol Si m^{-2} . If production of new BSi in the surface is equal to this supply term annually, BSi production for summer 2009 was ~ 0.35 mol Si m^{-2} .

However, as some accumulation of BSi had occurred prior to the onset of sampling, this figure is a minimum estimate. Initial values of BSi were ~ 8 μM , somewhat less than the February peak of 10 μM . As the early productivity event was smaller in magnitude, it should represent less production than during the February maximum. Thus, doubling the initial

estimate represents a reasonable upper limit, resulting in a range of $0.35 - 0.70 \text{ mol Si m}^{-2} \text{ y}^{-1}$. Using the calculated BSi:POC ratio (0.15; Figure 6), this equates to C production as POC of $2.3 - 4.7 \text{ mol C m}^{-2} \text{ y}^{-1}$, ~20-40% of the total C drawdown of $12 \text{ mol C m}^{-2} \text{ y}^{-1}$ estimated by Henley et al., (this issue) for the same season. Our range compares well with primary productivity ($2.5 - 16 \text{ mol C m}^{-2}$; Vernet and Smith, 2006; for a growing season of 120 d, Vernet et al., 2008) and net community production ($-0.25 - 6.5 \text{ mol C m}^{-2}$, for a growing season of 120 d; Huang et al., 2012) estimated for the wider WAP shelf.

To contrast this intermediate-chlorophyll situation with more typical, high-chlorophyll seasons, average Si_d drawdown and mixed layer depths based on long-term RaTS data were taken from Clarke et al., (2008). These concentrations were used to estimate expected isotopic signatures, based on the regression of $\delta^{30}\text{Si}_d$ versus Si_d from 2009 data to give an f_{DEEP} value of 0.59 (full details in supplementary information). The average maximum winter MLD is 60 m for pre-2006 conditions (Clarke et al., 2008), giving an integrated contribution of $2.3 \text{ mol Si m}^{-2}$ from deep to WW, and the average depth of the pycnocline was 30 m. This suggests that in typical high-chlorophyll years, supply of Si (and therefore new BSi production) is $\sim 1.2 \text{ mol Si m}^{-2} \text{ y}^{-1}$.

The estimate of BSi production in the low-chlorophyll conditions of summer 2009 represents a large (40–70%) reduction compared to the estimate for typical high-chlorophyll seasons. This is in keeping with the reductions in average chlorophyll (summer 2009 was 45% lower than the 2004-2006 average) and integrated seasonal chlorophyll (50–55% lower in 2009 than high-chlorophyll years; Annett 2013). The similar reductions in BSi, chlorophyll and C are consistent with the strong BSi:chlorophyll and BSi:POC relationships identified here. As recent studies have indicated a climate-induced shift towards lower chlorophyll conditions progressing southward along the WAP, this is expected to impact Si cycling.

4.5 Implications for Si cycling

The intense warming and strong decrease in chlorophyll in the northern areas of the WAP (Montes-Hugo et al., 2009) suggest that, as warming progresses, more areas will experience a decline in phytoplankton production. As this decrease results from changes in diatom communities, it will strongly impact the extent of opal production and Si cycling. The annual Si budget for 2009 reflects a year with relatively low chlorophyll compared with the long-term mean, and variation in new opal production (and export) and variations in

chlorophyll between seasons are of similar magnitude. If warming and sea-ice retreat progress southwards, new seasonal ice zones may follow the same trend towards lower productivity documented in the northern WAP region (Montes-Hugo et al., 2009), reducing BSi production and export.

Supply of Si to Ryder Bay is related to mixing from below with deeper, Si-rich waters, balanced by dilution from low-salinity meltwater inputs. Deeper mixing associated with continued reductions in winter sea-ice cover would act to increase Si_d in surface waters by incorporating deeper water with greater Si_d content. At a regional scale, the suggested increased frequency of UCDW incursions, bringing high-nutrient waters onto the WAP shelf (Martinson et al., 2008), would also act to increase Si_d to deeper source water (mCDW).

Over long time scales, such as those relevant to the interpretation of sediment records and paleoreconstructions, greater supply and reduced drawdown would lead to Si accumulation in waters along the WAP. As the WAP region is linked to other adjacent waters (Hofmann et al., 1996, Zhou et al., 2002, Savidge and Amft 2009), some of this Si-enriched water could eventually move into the open Southern Ocean, where Si is currently not fully utilised, representing a mechanism to increase Southern Ocean Si fluxes. In the Southern Ocean, Fe is the primary factor limiting phytoplankton growth, but north of the PFZ diatoms can be limited by low concentrations of Si (Brzezinski et al., 2005). Even south of the PFZ, co-limitation of diatom production by Fe and Si has been suggested (Leblanc et al., 2005; Hoffmann et al., 2008). Increased Si in the PFZ could be used both in the south and north by diatoms, or may be entrained into Antarctic Intermediate Water (AAIW). While Si in AAIW would not be immediately available to phytoplankton, this is a key mechanism distributing macronutrients to low-latitude regions, and thus could eventually increase diatom production in more temperate waters (similar to the Silicic Acid Leakage Hypothesis of Brzezinski et al., 2002). The scenario above, of increases in Si supply to Southern Ocean waters, could help to enhance currently limited productivity in the PFZ and eventually in low-latitude waters. While such an effect would be manifest only over long time scales, this is an additional mechanism bringing Si to the Southern Ocean, in addition to changes in circulation or overturning.

5. Conclusions:

The RaTS programme has shown that chlorophyll patterns in Ryder Bay are broadly typical of coastal polar regions, with a period of elevated summer production relative to low winter levels. The data presented here show that these trends are also reflected in Si drawdown and BSi production. Isotopic data reflect gradual, slight drawdown of Si, as seen in the enrichment of $\delta^{30}\text{Si}_d$ during the study season. Lighter signatures are found at depth, consistent with lower utilisation and potentially some release of Si from remineralisation. Estimated biological fractionation factors are -1.2 ‰ and -1.9 ‰ for closed and open systems, respectively. Given the small range of values here we are unable to discriminate between the two systems, but both estimates are highly consistent with those found for a previous Southern Ocean study (Varela et al., 2004).

Diatom speciation can potentially affect ϵ , and the data presented here suggest that *Chaetoceros* species, especially their resting spores, and *Coscinodiscus* species may have ϵ values higher than the bulk community average. Within our ability to resolve Si isotopes, these effects are minor relative to seasonal trends in surface waters. However, *Chaetoceros* species are often a significant component of sedimentary diatom assemblages, such that complementary diatom assemblage data must be taken into account when interpreting sedimentary $\delta^{30}\text{Si}$ as a proxy for Si drawdown (Sutton et al., 2013).

Combining Si concentrations and isotopic signatures with mixed layer depths, annual Si production of 0.35-0.70 mol Si m⁻² y⁻¹ was calculated for Ryder Bay for 2009-2010. This is considerably lower (40–70% lower) than the estimate for conditions typical of high-chlorophyll years. A continued shift to a warmer climate could potentially result in the increased occurrence of low-chlorophyll conditions in this region, and this would act to reduce BSi production, lowering Si_d drawdown in surface waters along the WAP. In combination with potential increases in Si supply, this presents a mechanism to redistribute unused Si from WAP shelf waters to the open Southern Ocean. This additional Si could stimulate Southern Ocean diatom growth where it is currently Si-limited, or it could be transported to temperate latitudes via AAIW, similar to the Silicic Acid Leakage Hypothesis.

Acknowledgements

We are grateful for the sampling opportunity and support from the RaTS programme, a component of the BAS Polar Oceans programme funded by the UK's Natural Environment Research Council (NERC), and the help from Rothera Station staff, especially the marine assistants. Funding for this project was provided by NERC, via Antarctic Funding Initiative 4/02, and Collaborative Gearing Scheme grants 10/50 and 11/56. The Captain, PI and crew of ARSV *Lawrence M. Gould* kindly allowed sample collection during the annual CTD intercalibration cruise. We thank Dr. Ben Reynolds at ETH-Zurich for providing training to ALA (funded by a GEOTRACES CostACTION Short Term Scientific Mission) and performing isotopic analyses. Laetitia Pichevin gave helpful discussion during writing. ALA was funded by scholarships from Natural Science and Engineering Research Council of Canada (PGSD-374281-2009) and the Overseas Research Students Awards Scheme and School of GeoSciences at the University of Edinburgh. We are grateful to the editor and two anonymous reviewers for their help in improving this manuscript.

References:

- Annett, A. L. 2013. *Diatom ecology and biogeochemistry of the warming Antarctic sea-ice zone*. PhD Thesis: University of Edinburgh.
- Annett, A.L., Carson, D.S., Crosta, X., Clarke, A. and Ganeshram, R.S. 2010. Seasonal progression of diatom assemblages in surface waters of Ryder Bay, Antarctica. *Polar biology*, **33**, 13–29, doi:10.1007/s00300-009-0681-7.
- Atkinson, A., Siegel, V., Pakhomov, E. and Rothery, P. 2004. Long-term decline in krill stock and increase in salps within the Southern Ocean. *Nature*, **432**, 100–103.
- Beucher, C.P., Brzezinski, M.A. and Crosta, X. 2007. Silicic acid dynamics in the glacial sub-Antarctic: Implications for the silicic acid leakage hypothesis. *Global Geochemical Cycles*, **21**, 1–13, doi:10.1029/2006GB002746.
- Beucher, C.P., Brzezinski, M.A. and Jones, J.L. 2011. Mechanisms controlling silicon isotope distribution in the Eastern Equatorial Pacific. *Geochimica et Cosmochimica Acta*, **75**, 4286–4294, doi:10.1016/j.gca.2011.05.024.
- Brzezinski, M. and Nelson, D.M. 1989. Seasonal change in the silicon cycle within a Gulf Stream warm-core ring. *Deep-Sea Research*. **36**(7): 1009-1030. doi:10.1016/0198-0149(89)90075-7.
- Brzezinski, M., Jones, J.L. and Demarest, M.S. 2005. Control of silica production by iron and silicic acid during the Southern Ocean Iron Enrichment Experiment (SOFEX). *Limnology and Oceanography*, **50**, 810–824.
- Brzezinski, M.A., Pride, C.J., Franck, V.M., Sigman, D.M., Sarmiento, J.L. and Matsumoto, K. 2002. A switch from Si(OH)_4 to NO_3^- depletion in the glacial Southern Ocean. *Geophysical Research Letters*, **29**, doi:10.1029/2001GL014349.
- Cardinal, D., Alleman, L.Y., Dehairs, F., Savoye, N., Trull, T.W. and André, L. 2005. Relevance of silicon isotopes to Si-nutrient utilization and Si-source assessment in Antarctic waters. *Global Biogeochemical Cycles*, **19**, 1–13, doi:10.1029/2004GB002364.
- Cardinal, D., Savoye, N., Trull, T.W., Dehairs, F., Kopczynska, E.E., Fripiat, F., Tison, J.-L. and André, L. 2007. Silicon isotopes in spring Southern Ocean diatoms: Large zonal changes despite homogeneity among size fractions. *Marine Chemistry*, **106**, 46–62, doi:10.1016/j.marchem.2006.04.006.
- Carson, D.S. 2008. *Biogeochemical Controls on Productivity and Particle Flux in the Coastal Antarctic Sea Ice Environment*. PhD Thesis: University of Edinburgh.

- Clarke, A., Meredith, M.P., Wallace, M.I., Brandon, M.A. and Thomas, D.N. 2008. Seasonal and interannual variability in temperature, chlorophyll and macronutrients in northern Marguerite Bay, Antarctica. *Deep Sea Research Part II: Topical Studies in Oceanography*, **55**, 1988–2006, doi:10.1016/j.dsr2.2008.04.035.
- Closset, I., Cardinal, D., Bray, S.G., Thil, F., Djouraev, I., Rigual-hernández, A.S., Trull, T.W., 2015. Seasonal variations, origin, and fate of settling diatoms in the Southern Ocean tracked by silicon isotope records in deep sediment traps. *Global Biogeochem. Cycles* 29, 1495–1510. doi:10.1002/2015GB005180.
- Coffineau, N., De La Rocha, C.L. and Pondaven, P. 2014. Exploring interacting influences on the silicon isotopic composition of the surface ocean: a case study from the Kerguelen Plateau. *Biogeosciences*, **11**, 1371–1391, doi:10.5194/bg-11-1371-2014.
- De La Rocha, C.L. 2006. Opal-based isotopic proxies of paleoenvironmental conditions. *Global Biogeochemical Cycles*, **20**, doi:10.1029/2005GB002664.
- De La Rocha, C.L., Brzezinski, M.A. and DeNiro, M.J. 1997. Fractionation of silicon isotopes by marine diatoms during biogenic silica formation. *Geochimica et Cosmochimica Acta*, **61**, 5051–5056.
- De La Rocha, C.L., Brzezinski, M.A., DeNiro, M.J. and Shemesh, A. 1998. Silicon-isotope composition of diatoms as an indicator of past oceanic change. *Nature*, **395**, 680–683.
- Demarest, M.S., Brzezinski, M.A. and Beucher, C.P. 2009. Fractionation of silicon isotopes during biogenic silica dissolution. *Geochimica et Cosmochimica Acta*, **73**, 5572–5583, doi:10.1016/j.gca.2009.06.019.
- de Souza, G.F., Slater, R.D., Dunne, J.P. and Sarmiento, J.L. 2014. Deconvolving the controls on the deep ocean's silicon stable isotope distribution. *Earth and Planetary Science Letters*. **298**: 66–76. doi:10.1016/j.epsl.2014.04.040.
- de Souza, G.F., Reynolds, B.C., Rickli, J., Frank, M., Saito, M.A., Gerringa, L.J.A., Bourdon, B., 2012. Southern Ocean control of silicon stable isotope distribution in the deep Atlantic Ocean. *Global Biogeochem. Cycles* 26, 1–13. doi:10.1029/2011GB004141.
- Ellwood, M.J., Wille, M. and Maher, W. 2010. Glacial silicic acid concentrations in the Southern Ocean. *Science*, **330**, 1088–1091, doi:10.1126/science.1194614.
- Egan, K.E., Rickaby, R.E.M., Leng, M.J., Hendry, K.R., Hermoso, M., Sloane, H.J., Bostock, H. and Halliday, A.N. 2012. Diatom silicon isotopes as a proxy for silicic acid utilization: A Southern Ocean core top calibration. *Geochimica et Cosmochimica Acta*, **96**, 174–192,

doi:10.1016/j.cga.2012.08.002.

Fripiat, F., Cavagna, A.-J., Savoye, N., Dehairs, F., André, L. and Cardinal, D. 2011. Isotopic constraints on the Si-biogeochemical cycle of the Antarctic Zone in the Kerguelen area (KEOPS). *Marine Chemistry*, **123**, 11–22, doi:10.1016/j.marchem.2010.08.005.

Fripiat, F., Cavagna, A., Dehairs, F., Brauwere, A. De, Andre, L., Cardinal, D., 2012. Processes controlling the Si-isotopic composition in the Southern Ocean and application for paleoceanography. *Biogeosciences* 9, 2443–2457. doi:10.5194/bg-9-2443-2012

Garibotti, I.A., Vernet, M. and Ferrario, M.E. 2005. Annually recurrent phytoplanktonic assemblages during summer in the seasonal ice zone west of the Antarctic Peninsula (Southern Ocean). *Deep Sea Research Part I: Oceanographic Research Papers*, **52**, 1823–1841, doi:10.1016/j.dsr.2005.05.003.

Garrison, D.L. 1984. Planktonic diatoms. In Steindinger, K.A., ed. *Marine Plankton Life Cycle Strategies*. Boca Raton: CRC Press Inc., 1–17.

Georg, R.B., Reynolds, B.C., Frank, M. and Halliday, A.N. 2006. New sample preparation techniques for the determination of Si isotopic compositions using MC-ICPMS. *Chemical Geology*, **235**, 95–104, doi:10.1016/j.chemgeo.2006.06.006.

Gnanadesikan, A. and Toggweiler, J.R. 1999. Constraints placed by silicon cycling on vertical exchange in general circulation models. *Geophysical Research Letters*, **26**, 1865–1868.

Hasle, G.R. and Syvertsen, E.E. 1997. Marine Diatoms. In Tomas, C.R., ed. *Identifying marine phytoplankton*, San Diego: Academic Press, 5-385.

Hendry, K.R., Robinson, L.F., McManus, J.F. and Hays, J.D. 2014a. Silicon isotopes indicate enhanced carbon export efficiency in the North Atlantic during deglaciation. *Nature Communications*. **5**: 3107. doi:10.1038/ncomms4107.

Hendry, K.R. and Brzezinski, M.A. 2014b. Using silicon isotopes to understand the role of the Southern Ocean in modern and ancient biogeochemistry and climate. *Quaternary Science Reviews*. **89**: 13-26. doi:10.1016/j.quascirev.2014.01.019.

Henley, S.F. 2012. *Climate-induced changes in carbon and nitrogen cycling in the rapidly warming Antarctic coastal ocean*. PhD Thesis: University of Edinburgh.

Henley, S.F., Annett, A.L., Ganeshram, R.S, Carson, D.S., Weston, K., Crosta, X., Tait, A., Dougans, J., Fallick, A.E. and Clarke, A. 2012. Factors influencing the stable carbon isotopic composition of suspended and sinking organic matter in the coastal Antarctic sea ice environment. *Biogeosciences*, **9**, 1137-1157. doi:10.5194/bg-9-1137-2012.

716 Hildebrand, M. 2008. Diatoms, Biomineralization Processes, and Genomics. *Chemical*
717 *Reviews*, **108**, 4855–4874, doi:10.1021/cr078253z.

718 Hillebrand, H., Durselen, C.-D., Kirschtel, D., Pollinger, U. and Zohary, T. 1999. Biovolume
719 calculation for pelagic and benthic microalgae. *Journal of Phycology*, **35**, 403-424.

720 Hoffmann, L.J., Peeken, I. and Lochte, K. 2008. Iron, silicate, and light co-limitation of three
721 Southern Ocean diatom species. *Polar biology*, **31**, 1067–1080, doi:10.1007/s00300-008-
722 0448-6.

723 Hofmann, E.E., Klinck, J.M., Lascara, C.M. and Smith, D.A. 1996. Water mass distribution
724 and circulation west of the Antarctic Peninsula and including Bransfield Strait. *Antarctic*
725 *Research Series: Foundations for ecological research west of the Antarctic Peninsula*,
726 **70**, 61–80.

727 Holm-Hansen, O., Mitchell, B.G., Hewes, C.D. and Karl, D.M. 1989. Phytoplankton blooms
728 in the vicinity of Palmer Station, Antarctica. *Polar biology*, **10**, 49:57.

729 Huang, K., Ducklow, H., Vernet, M., Cassar, N. and Bender, M.L. 2012. Export production
730 and its regulating factors in the West Antarctic Peninsula region of the Southern Ocean.
731 *Global Biogeochemical Cycles*, **26**, GB2005, doi:10.1029/2010GB004028.

732 Jacobs, S.S. 1991. On the nature and significance of the Antarctic Slope Front. *Marine*
733 *Chemistry*, **35**, 9–24, doi:10.1016/S0304-4203(09)90005-6.

734 Klinck, J.M. 1998. Heat and salt changes on the continental shelf west of the Antarctic
735 Peninsula between January 1994 and January 1994. *Journal of Geophysical Research*,
736 **103**, 7617–7636.

737 Leblanc, K., Hare, C.E., Boyd, P.W., Bruland, K.W., Sohst, B., Pickmere, S., Lohan, M.C.,
738 Buck, K., Ellwood, M. and Hutchins, D.A. 2005. Fe and Zn effects on the Si cycle and
739 diatom community structure in two contrasting high and low-silicate HNLC areas. *Deep*
740 *Sea Research Part I: Oceanographic Research Papers*, **52**, 1842–1864,
741 doi:10.1016/j.dsr.2005.06.005.

742 Leventer, A., Domack, E., Barkoukis, A., McAndrews, B. and Murray, J. 2002. Laminations
743 from the Palmer Deep: A diatom-based interpretation. *Paleoceanography*, **17**, 8002,
744 doi:10.1029/2001PA000624.

745 Loeb, V., Siegel, V., Holm-Hansen, O., Hewitt, R., Fraser, W., Trivelpiece, W. and
746 Trivelpiece, S. 1997. Effects of sea-ice extent and krill or salp dominance on the
747 Antarctic food web. *Nature*, **387**.

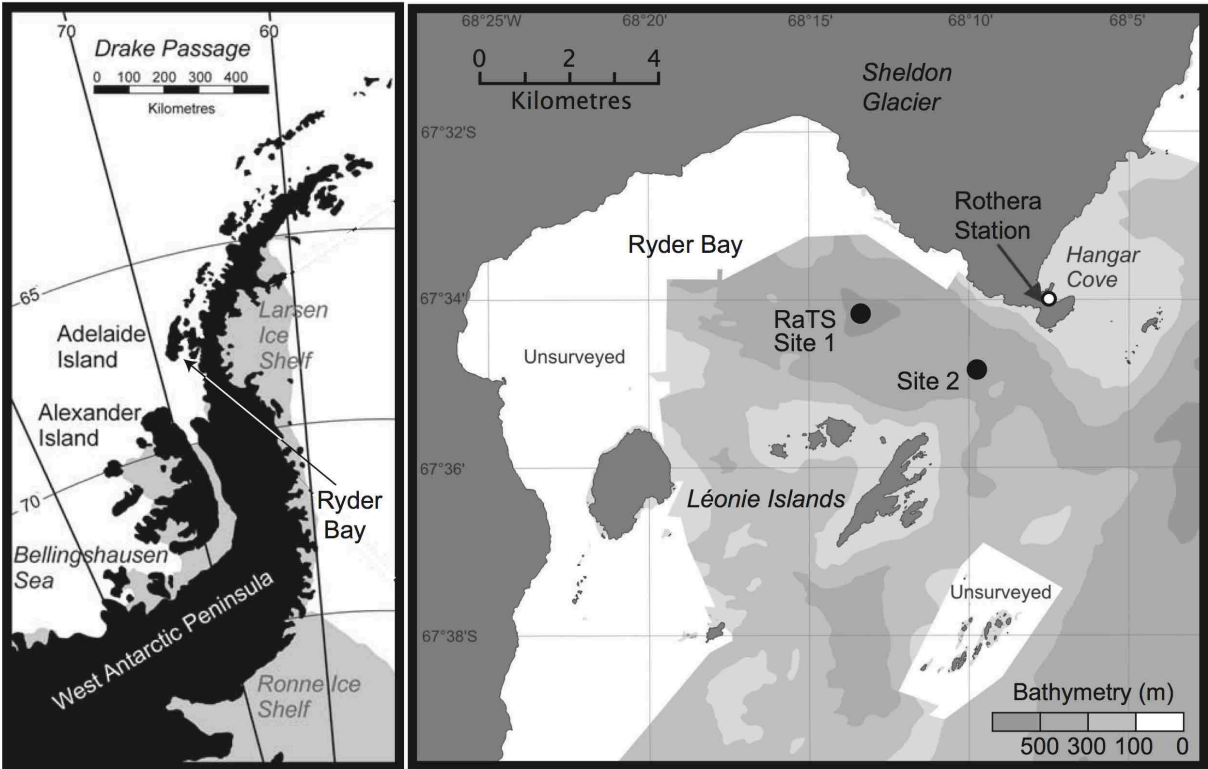
- Marchetti, A. and Cassar, N. 2009. Diatom elemental and morphological changes in response to iron limitation: a brief review with potential paleoceanographic applications. *Geobiology*, **7**, 419–431, doi:10.1111/j.1472-4669.2009.00207.
- Martin-Jézéquel, V., Hildebrand, M. and Brzezinski, M.A. 2000. Silicon metabolism in diatoms: Implications for growth. *Journal of Phycology*, **36**, 821.
- Martinson, D.G., Stammerjohn, S.E., Iannuzzi, R.A., Smith, R.C. and Vernet, M. 2008. Western Antarctic Peninsula physical oceanography and spatio-temporal variability. *Deep-Sea Research II*, **55**, 1964–1987, doi:10.1016/j.dsr2.2008.04.038.
- Massom, R.A. and Stammerjohn, S.E. 2010. Antarctic sea ice change and variability – Physical and ecological implications, *Polar Science*, **4**(2), 149–186, doi:10.1016/j.polar.2010.05.001.
- Matsumoto, K., Sarmiento, J.L. and Brzezinski, M.A. 2002. Silicic acid leakage from the Southern Ocean: A possible explanation for glacial atmospheric $p\text{CO}_2$. *Global Biogeochemical Cycles*, **16**, 1–23, doi:10.1029/2001GB001442.
- Meredith, M.P. and King, J.C. 2005. Rapid climate change in the ocean west of the Antarctic Peninsula during the second half of the 20th century. *Geophysical Research Letters*. **32**(19): L19604, doi: 10.1029/2005GL024042.
- Meredith, M.P., Renfrew, I.A., Clarke, A., King, J.C. and Brandon, M.A. 2004. Impact of the 1997/98 ENSO on upper ocean characteristics in Marguerite Bay, western Antarctic Peninsula. *Journal of Geophysical Research*, **109**, doi:10.1029/2003JC001784.
- Meredith, M.P., Wallace, M.I., Stammerjohn, S.E., Renfrew, I.A., Clarke, A., Venables, H.J., Shoosmith, D.R., Souster, T. and Leng, M.J. 2010. Changes in the freshwater composition of the upper ocean west of the Antarctic Peninsula during the first decade of the 21st century. *Progress In Oceanography*, **87**, 127–143, doi:10.1016/j.pocean.2010.09.019.
- Milligan, A.J., Varela, D.E., Brzezinski, M.A. and Morel, F.M.M. 2004. Dynamics of silicon metabolism and silicon discrimination in a marine diatom as a function of $p\text{CO}_2$. *Limnology and Oceanography*, **49**, 322–329.
- Montes-Hugo, M., Doney, S.C., Ducklow, H.W., Fraser, W., Martinson, D., Stammerjohn, S.E. and Schofield, O. 2009. Recent Changes in Phytoplankton Communities Associated with Rapid Regional Climate Change Along the Western Antarctic Peninsula. *Science*, **323**, 1470–1473, doi:10.1126/science.1164533.

- Nelson, D.M., Brzezinski, M.A., Sigman, D.E. and Franck, V.M. 2001. A seasonal progression of Si limitation in the Pacific sector of the Southern Ocean. *Deep-Sea Research II*, **48**, 3973–3995.
- Nelson, D.M., Tréguer, P., Brzezinski, M.A., Leynaert, A. and Quéguiner, B. 1995. Production and dissolution of biogenic silica in the ocean: Revised global estimates, comparison with regional data and relationship to biogenic sedimentation. *Global Biogeochemical Cycles*, **9**, 359–372.
- Pichevin, L., Ganeshram, R.S., Ben C Reynolds, Prahl, F., Pedersen, T.F., Thunell, R. and McClymont, E.L. 2012. Silicic acid biogeochemistry in the Gulf of California: Insights from sedimentary Si isotopes. *Paleoceanography*, **27**, 1–14, doi:10.1029/2011PA002237.
- Pichevin, L.E., Reynolds, B.C., Ganeshram, R.S., Cacho, I., Pena, L., Keefe, K. and Ellam, R.M. 2009. Enhanced carbon pump inferred from relaxation of nutrient limitation in the glacial ocean. *Nature*, **459**, 1114–1117, doi:10.1038/nature08101.
- Ragueneau, O. and Treguer, P. 1994. Determination of biogenic silica in coastal waters: applicability and limits of the alkaline digestion method. *Marine Chemistry*, **45**(1-2): 43–51. doi:10.1016/0304-4203(94)90090-6.
- Ragueneau, O., Savoye, N., Del Amo, Y., Cotten, J., Tardiveau, B. and Leynaert, A. 2005. A new method for the measurement of biogenic silica in suspended matter of coastal waters: using Si:Al ratios to correct for the mineral interference. *Continental Shelf Research*, **25**, 697–710, doi:10.1016/j.csr.2004.09.017.
- Reynolds, B.C. 2009. Modeling the modern marine $\delta^{30}\text{Si}$ distribution. *Global Biogeochemical Cycles*, **23**, doi:10.1029/2008GB003266.
- Reynolds, B.C., Frank, M. and Halliday, A.N. 2006. Silicon isotope fractionation during nutrient utilization in the North Pacific. *Earth and Planetary Science Letters*, **244**, 431–443, doi:10.1016/j.epsl.2006.02.002.
- Rintoul, S.R. and Trull, T.W. 2001. Seasonal evolution of the mixed layer in the Subantarctic Zone south of Australia. *Journal of Geophysical Research*, **106**, 31447–31462.
- Saba, G.K., Fraser, W.R., Saba, V.S., Iannuzzi, R.A., Coleman, K.E., Doney, S.C., Ducklow, H.W., Martinson, D.G., Miles, T.N., Patterson-Fraser, D.L., Stammerjohn, S.E., Steinberg, D.K. and Schofield, O.M. 2014. Winter and spring controls on the summer food web of the coastal West Antarctic Peninsula, *Nature Communications*, **5**, doi:10.1038/ncomms5318.

- Sarmiento, J.L., Gruber, N., Brzezinski, M.A. and Dunne, J.P. 2004. High-latitude controls of thermocline nutrients and low latitude biological productivity. *Nature*, **427**, 56–60.
- Sarmiento, J.L., Simeon, J., Gnanadesikan, A., Gruber, N., Key, R.M. and Schlitzer, R. 2007a. Deep ocean biogeochemistry of silicic acid and nitrate. *Global Biogeochemical Cycles*, **21**, 10.1029/%5D2006GB002720.
- Savidge, D.K. and Amft, J.A. 2009. Circulation on the West Antarctic Peninsula derived from 6 years of shipboard ADCP transects. *Deep Sea Research Part I: Oceanographic Research Papers*, **56**, 1633–1655, doi:10.1016/j.dsr.2009.05.011.
- Smayda, T.J. 1978. From phytoplankters to biomass. In Sournia, A. ed. *Monographs on oceanographic methodology*. Paris: UNESCO, 273-279.
- Sutton, J.N., Varela, D.E., Brzezinski, M.A. and Beucher, C.P. 2013. Species-dependent silicon isotope fractionation by marine diatoms. *Geochimica et Cosmochimica Acta*, **104**, 300-309, doi:10.1016/j.cga.2012.10.057.
- Thamatrakoln, K. and Hildebrand, M. 2008. Silicon uptake in diatoms revisited: a model for saturable and nonsaturable uptake kinetics and the role of silicon transporters. *Plant physiology*, **146**:(3), 1397-1407.
- Vaughan, D.G., Marshall, G.J., Connolley, W.M., Parkinson, C., Mulvaney, R., Hodgson, D.A., King, J.C., Pudsey, C.J. and Turner, J. 2003. Recent rapid regional climate warming on the Antarctic Peninsula. *Climatic Change*, **60**, 243–274.
- Varela, M., Fernandez, E. and Serret, P. 2002. Size-fractionated phytoplankton biomass and primary production in the Gerlache and south Bransfield Straits (Antarctic Peninsula) in Austral summer 1995-1996. *Deep-Sea Research II*, **49**, 749–768.
- Varela, D.E., Pride, C.J. and Brzezinski, M.A. 2004. Biological fractionation of silicon isotopes in Southern Ocean surface waters. *Global Biogeochemical Cycles*, **18**, doi:10.1029/2003GB002140.
- Venables, H.J., Clarke, A. and Meredith, M.P. 2013. Wintertime controls on summer stratification and productivity at the western Antarctic Peninsula. *Limnology and Oceanography*. **58**:(3), 1035-1047.
- Venables, H.J. and Meredith, M.P. 2014. Feedbacks between ice cover, ocean stratification, and heat content in Ryder Bay, western Antarctic Peninsula. *Journal of Geophysical Research: Oceans*, **119**, 5323-5336, doi:10.1002/2013JC009669.
- Vernet, M., and Smith, R.C. .2006. Measuring and modeling primary production in marine

- pelagic ecosystems. In: Fahey, J., Knapp, A. (Eds). LTER Net Primary Production Methods. Oxford University Press, Oxford.
- Vernet, M., Martinson, D., Iannuzzi, R., Stammerjohn, S.E., Kozlowski W., Sines, K., Smith, R. and Garibotti, I. 2008. Primary production within the sea-ice zone west of the Antarctic Peninsula: I-Sea ice, summer mixed layer, and irradiance, *Deep-Sea Research Part II*, **55**:(18-19), 2068-2085, doi: 10.1016/j.dsr2.2008.05.021.
- Wallace, M. I., Meredith, M.P., Brandon, M.A., Sherwin, T.J., Dale, A. and Clarke, A. 2008. On the characteristics of internal tides and coastal upwelling behaviour in Marguerite Bay, west Antarctic Peninsula. *Deep-Sea Research II*, **55**, 2023–2040.
- Wetzel, F., de Souza, G.F. and Reynolds, B.C. 2014. What controls silicon isotope fractionation during dissolution of diatom opal? *Geochimica et Cosmochimica Acta*, **131**, 128-137, doi:10.1016/j.gca.2014.01.028
- Whitworth, T.I., Orsi, A.H., Kim, S.-J. and Nowlin, W.D. 1998. Water masses and mixing near the Antarctic slope front. *Antarctic Research Series*, **75**, 1–27.
- Wischmeyer, A.G., La Rocha, De, C.L., Maier-Reimer, E. and Wolf-Gladrow, D.A. 2003. Control mechanisms for the oceanic distribution of silicon isotopes. *Global Biogeochemical Cycles*, **17**, 1–12, doi:10.1029/2002GB002022.
- Yool, A. and Tyrell, T. 2003. Role of diatoms in regulating the ocean's silicon cycle. *Global Biogeochemical Cycles*, **17**, doi:10.1029/2002GB002018.
- Zhou, M., Niiler, P.P. and Hu, J.-H. 2002. Surface currents in the Bransfield and Gerlache Straits, Antarctica. *Deep-Sea Research I*, **49**, 267–280.

866 **Figures and captions:**



867
868 Figure 1: Location and bathymetry of Ryder Bay, showing the RaTS sampling sites and
869 location of Rothera Research Station.

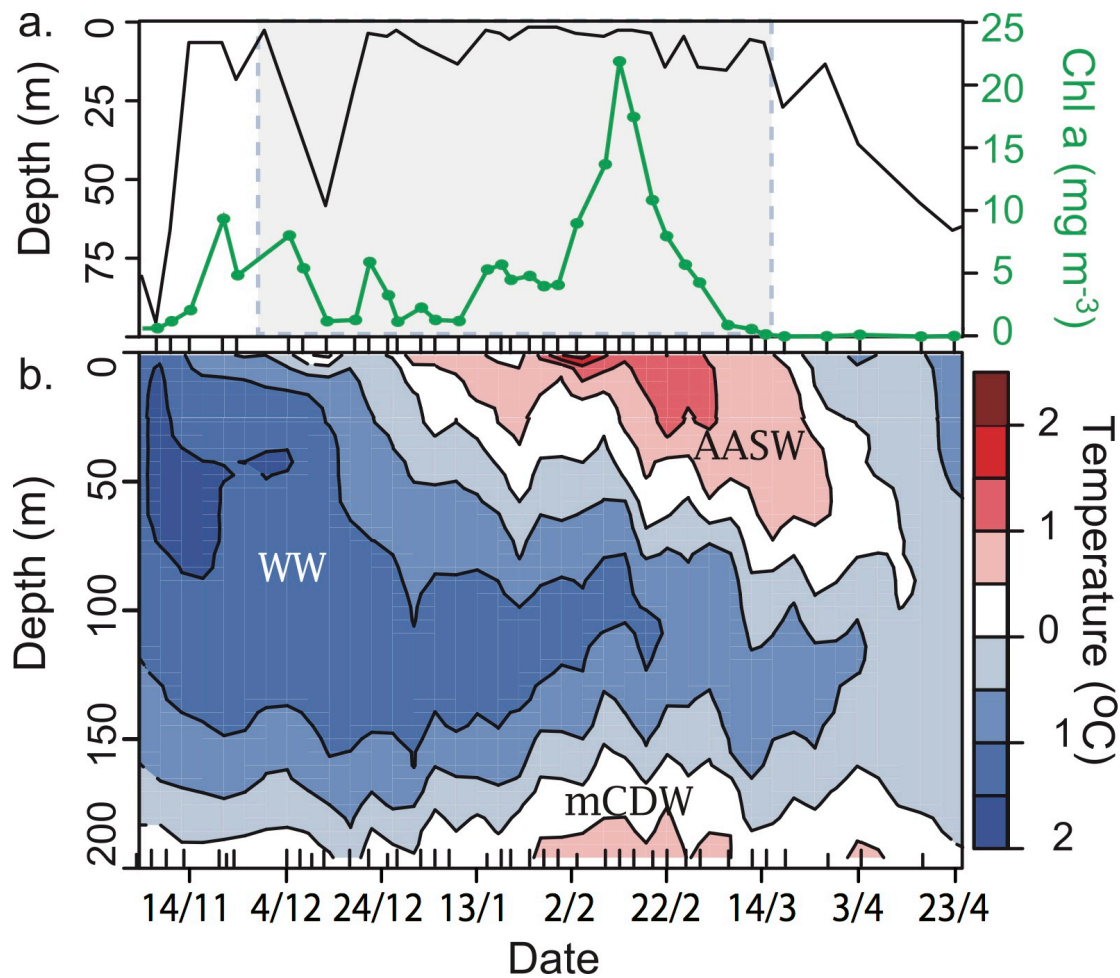


Figure 2: (a) MLD and chlorophyll at 15 m, with the shaded region indicating the sampling period for Si work. (b) Temperature in the top 200 m, labels denote properties associated with winter water (WW), Antarctic surface water (AASW) and modified Circumpolar Deep Water (mCDW). Inward tick marks on the x-axis show sampling events.

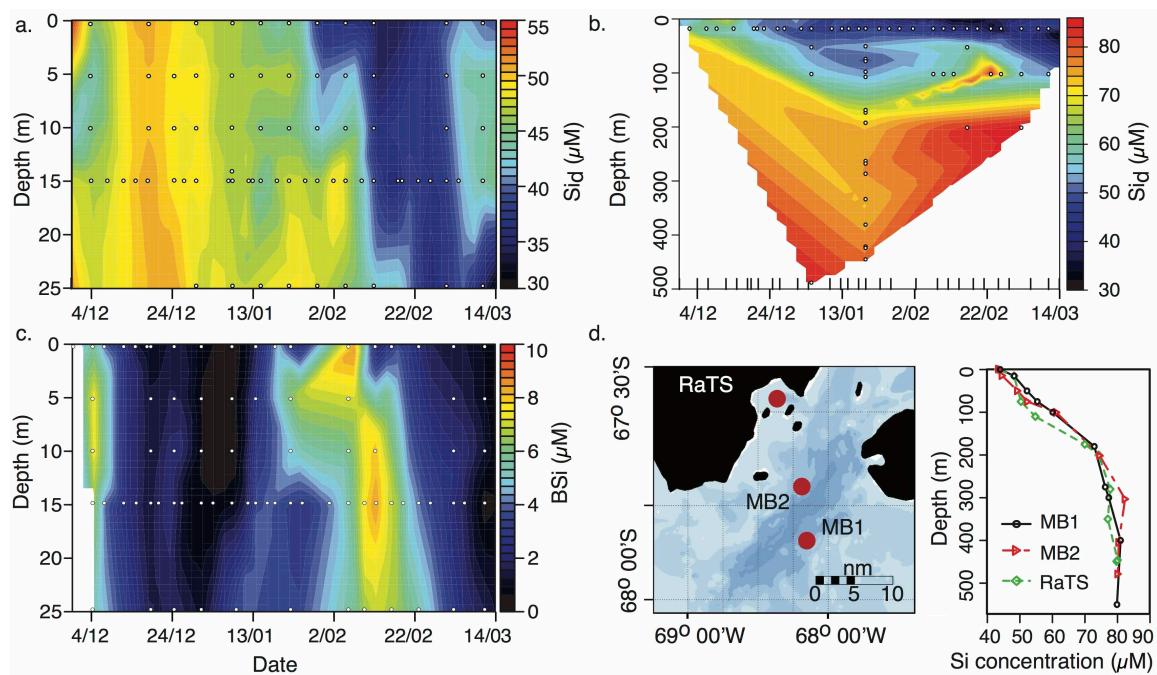


Figure 3: Surface (a; 0–25 m) and deep water (b) concentrations of Si_d , and (c) surface concentrations of BSi at the RaTS site (Ryder Bay). Panel (d) shows locations and Si_d at three sites in Marguerite and Ryder Bays. Filled symbols denote sampling depths and events.

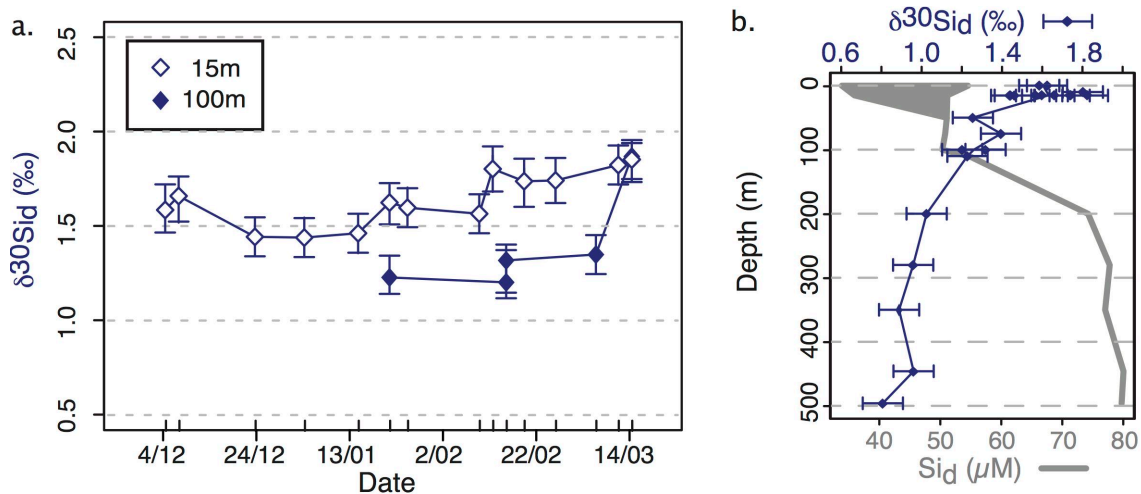


Figure 4: Si isotopic composition from time-series samples at 15 m and 100–110 m (a; open and closed symbols, respectively) and all depths (b). Also shown in (b) is Si_d concentration with depth. Error bars represent one standard deviation.

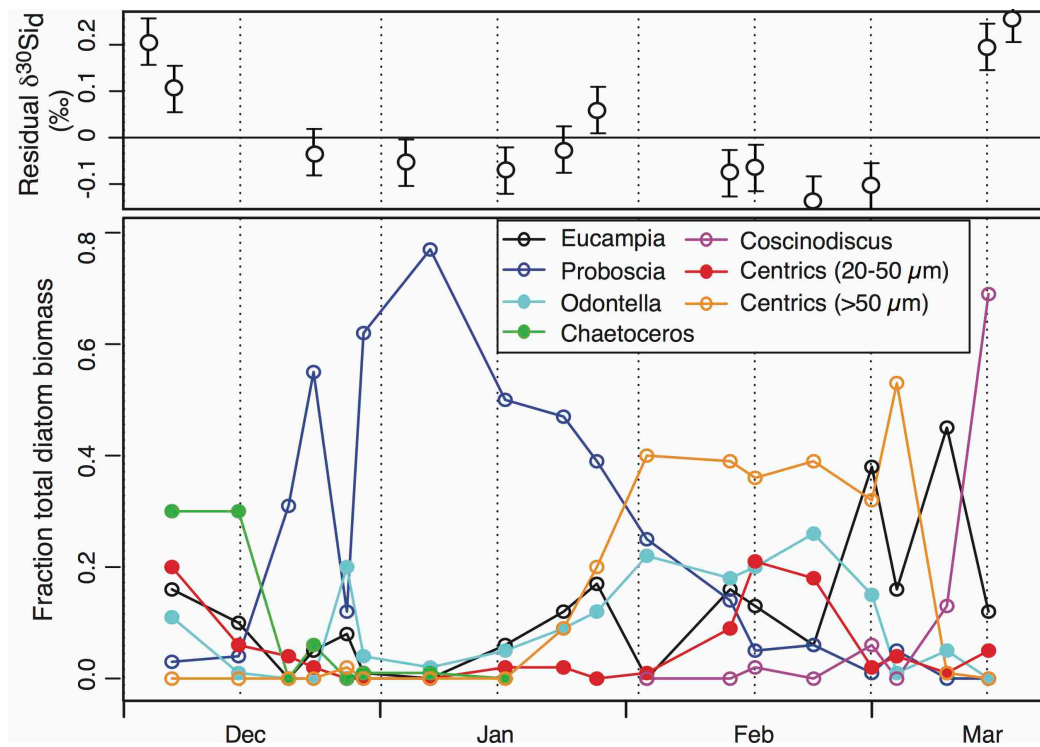


Figure 5: Time-series plot of residual $\delta^{30}\text{Si}_d$ (difference between measured and expected values) and key diatom species as fraction of total diatom biomass. Species shown are *Eucampia antarctica*, *Proboscia inermis*, *Odontella weissflogii*, *Chaetoceros* (*Hyalochaeta* subgenus), *Coscinodiscus* spp., and medium (20-50 μm) and large (>50 μm) discoid centric species.

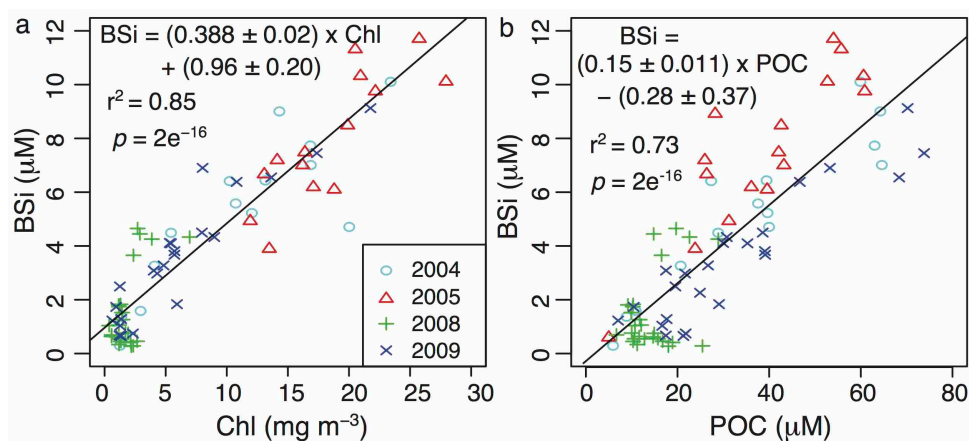


Figure 6: Particulate Si versus (a) chl and (b) POC for 4 seasons at the RaTS site. Data from 2004 and 2005 are total particulate Si, 2008 and 2009 are BSi. A linear regression model (solid line) is shown for both relationships, using all four years' data. Despite the inclusion of lithogenic Si in 2004 and 2005 samples, individual season regressions (not shown) are all statistically significant ($p < 0.05$) and in each case are consistent with the overall relationship. All samples are from 15 m.

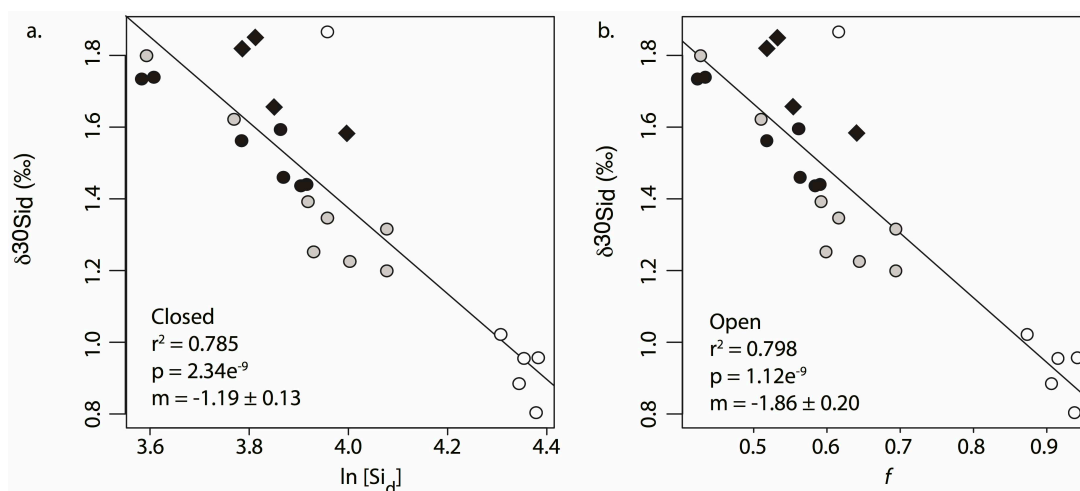


Figure 7: Least-squares fit to the data for closed (left) and open (right) fractionation (excluding 18 March sample at 100m). Over this range the two systems are virtually indistinguishable. For a closed system, isotopic signature is plotted versus $\ln[\text{Si}_d]$, whereas for an open system $\delta^{30}\text{Si}_d$ is plotted versus fraction remaining (f), defined as $[\text{Si}_d]/[\text{Si}_d]_{\text{initial}}$. Shading reflects depth, with black symbols being shallow (<25 m), grey 50-100 m, and open symbols deep water (>200 m). Diamonds indicate surface water samples discussed in section 4.2.

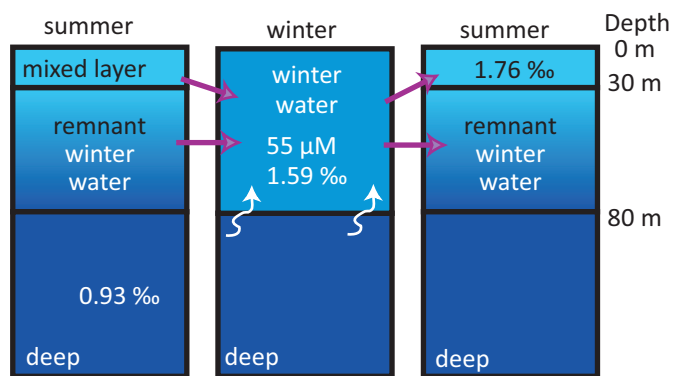


Figure 8: Schematic showing mixing of the water masses in the one-dimensional model used here to estimate seasonal Si demand. Values used in the model are indicated on each water mass: isotopic composition for all, and $[\text{Si}_d]$ for WW.

Supplementary information:

To calculate a Si budget for 2009 using the model described by Fripiat et al., (2011), the isotopic signature of three water masses was required, along with the Si_d winter water, and depth of mixing in both winter and summer. All values used are listed in Table S1, and the rationale for each value is described here.

The first sample collected from the 2009 season was used as a best approximation of WW conditions (55 μM , 1.585 ‰), although there is evidence that there had been some BSi production already, thus this will underestimate total BSi production. Samples from 15 Feb to 1 March were averaged for the most depleted end-member (1.76 ‰), as they spanned the seasonal minimum in Si_d . Average deep-water values of 0.93 ‰ were used for the high-Si end-member. As noted in the main text, the fractional contribution of deep Si-rich waters to the WW layer (f_{DEEP}) was calculated following the equation in Fripiat et al., (2011):

$$f_{DEEP} = \frac{\delta^{30}Si_d^{WW} - \delta^{30}Si_d^{SML}}{\delta^{30}Si_d^{DW} - \delta^{30}Si_d^{SML}} \quad (3)$$

where superscripts refer to winter water (WW), summer mixed layer (SML) and deep waters (DW). This resulted in an f_{DEEP} of 0.21 for 2009.

The depth of the winter mixed layer was taken as 80 m, from late-winter CTD data. During the period of maximum drawdown (February 15 to March 1) used for calculation of average $\delta^{30}Si_d^{SML}$, CTD data indicate a pycnocline at ~30 m, in agreement with the relatively consistent Si_d throughout the top 25 m sampled (Figure 3a).

For an estimated Si budget representative of more typical, high-chlorophyll seasons, typical Si_d concentrations were taken from Clarke et al., (2008), where WW Si_d is ~65 μM , and summer minima occur in March, averaging 50 μM . Using the strong regression found here for $\delta^{30}Si_d$ versus Si_d (Figure S1), these concentrations were used to calculate the expected isotopic signatures of WW and SML in typical high-chl conditions. This gave -1.13 and -1.43 ‰ for WW and SML, respectively, and combined with the deep water value (which was assumed not to change annually) resulted in a typical f_{DEEP} value of 0.59.

Further, the average maximum winter MLD for pre-2006 conditions, taken from Clarke et al., 2008, was 60 m. This value combined with an f_{DEEP} of 0.59 gives an integrated contribution of 2.3 mol Si m^{-2} from deep to WW. As for 2009, temperature and density profiles were evaluated for the period of summer minimum Si_d , and the average depth of the

pycnocline, above which Si_d is likely to be consistent, was 30 m (range 20 – 40 m). These values gave an overall estimate of Si supply (equal to new BSi production) of $\sim 1.2 \text{ mol Si m}^{-2} \text{ y}^{-1}$ for typical high-chlorophyll years at the RaTS site.

Table S1: Values used for estimating seasonal Si production.

Parameter	Value for 2009	Value for typical, high-chl years
$\delta^{30}\text{Si}_d^{\text{WW}}$	1.59 ‰	1.13 ‰
$\delta^{30}\text{Si}_d^{\text{DW}}$	0.93 ‰	0.93 ‰
$\delta^{30}\text{Si}_d^{\text{SML}}$	1.76 ‰	1.43 ‰
f_{DEEP}	0.21	0.59
Si_d^{WW}	55 μM	65 μM
Depth^{WW}	80 m	60 m
Si_d from DW to WW	$0.93 \text{ mol Si m}^{-2}$	$2.3 \text{ mol Si m}^{-2}$
$\text{Depth}^{\text{SML}}$	30 m	30 m
Proportion WW entrained into SML	0.38 (= $30 \div 80$)	0.5 (= $30 \div 60$)
Si supplied to SML (annual, from WW)	$0.35 \text{ mol Si m}^{-2}$	$1.2 \text{ mol Si m}^{-2}$